Journal Name

ARTICLE

Theoretical study of the adsorption of hydrogen on cobalt clusters

Kevin García-Díez,[a] Julio Fernández-Fernández,[a] Julio A. Alonso[a,b] and María J. López[*a]

Adsorption and dissociation of molecular hydrogen on transition metal clusters are basic processes of broad technological application in fields such as catalysis, hydrogenation reactions, hydrogen fuel cells, hydrogen storage, etc. Here we focus on two cobalt clusters, Co_6 and Co_{13} and use the Density Functional Formalism to investigate: i) the mechanisms for adsorption and dissociation of hydrogen, and ii) the competition between the two processes as the amount of hydrogen increases towards cluster saturation. The dissociative adsorption of hydrogen is the preferred adsorption channel for low coverage. Each individual H atom binds to the cluster with an ionic type of bonding, similar to that in metal hydrides. The electronic levels of the H atoms hybridize with the deepest levels of the Co cluster, leading to the stabilization of the system. In contrast H_2 binds to the cluster with a weak covalent type of bond and the electronic density of the molecule becomes polarized. The electronic levels of the molecule are deeper than those of the Co cluster and do not hybridize with them, what explains the weak bonding of the molecule to the cluster. Interestingly, the high magnetic moments of the Co clusters do not change when H_2 is adsorbed in molecular form, but the magnetic moments are reduced by two units upon dissociative adsorption of the molecule. Adsorption and dissociation of H_2 on Co_6 and Co_{13} exhibit similar features, although the adsorption energies on Co_{13} are stronger. Saturation of Co_6 with hydrogen has been also investigated. Co_6 can adsorb up to four H_2 molecules in the dissociated form. Additional hydrogen is adsorbed in molecular form leading to a saturated cluster with sixteen hydrogen molecules, four dissociated and twelve molecular. This limit corresponds to a content of 8.4 wt% of hydrogen in the Co cluster, which is promising for the purpose of hydrogen storage .

A Introduction

The properties of metal clusters and nanoparticles usually change with the number of atoms in the cluster in a non-scalable way, and this feature motivates the interest in their study. The properties of clusters of simple metals are explained as due to the *sp* electrons forming electronic shells in a common confining effective potential.[1-2] Clusters of the transition metals are more complex, and their properties are dominated by the *d* electrons localized on the atoms.[3] Many works have focused on understanding the geometrical structure, that is, the arrangement of the atoms in the cluster.[3-11] Knowledge of the structure is useful to interpret the role of clusters and nanoparticles in catalysis, because the most active cluster atoms are usually those occupying the least coordinated surface sites.[12-13]

The interaction of hydrogen with metal clusters and nanoparticles plays an important role in several technological fields. Porous carbons are being investigated as possible hydrogen containers in electric cars using engines based on a

hydrogen fuel cell,[14] and experimental work indicates that doping with metal clusters and nanoparticles enhances the hydrogen storage capacity of the porous carbons.[15-17] For this reason, the interaction of H_2 with metal clusters and nanoparticles, in particular those of the 4*d* transition metals, has been investigated. Some theoretical calculations have focused on palladium,[18-20] concluding that the mechanism responsible for the enhancement of the storage capacity in the doped carbons is still not well understood.[20] The interaction between hydrogen and transition metal clusters is also relevant in the operation of the fuel cell. Transition metal clusters embedded in the anode of the fuel cell catalyze the dissociation of molecular hydrogen in protons (which go through a proton exchange membrane) and electrons (which go through an external electric circuit), that recombine with oxygen at the cathode of the fuel cell. In addition, hydrogen chemisorption on the surface of transition metals is a process of interest in heterogeneous catalysis. A number of transition metal surfaces and nanoparticles catalyze hydrogenation reactions, and these require the presence of adsorbed hydrogen atoms.

The 3*d* transition metals, because of their lower mass compared to the 4*d* metals, can be of interest for the applications mentioned above, and we focus attention on cobalt. This metal is present in many devices like cell phones, computers and video-cameras. It is also expected that Co will play an essential role in enlarging the useful life of lithium

batteries. The photoelectron spectra of anionic cobalt clusters, Co_n^-, with N = 1 – 108, have been measured by Liu et al.[21] The shape of the spectra varies with cluster size, especially for n<20. The magnetic moment of Co_n clusters produced in molecular beams was investigated by Billas et al,[22] revealing that clusters with sizes up to a few hundred atoms are more magnetic than bulk Co. The structure and magnetism of free Co clusters has been studied in several papers using the density functional theory (DFT),[9,23-26] and the properties of small Co clusters supported on graphene or graphene fragments have also been investigated.[27-29]

To explore the possibility of widening the applications of cobalt clusters and nanoparticles, it is of interest to study their interaction with hydrogen. Co surfaces catalyze the Fischer-Tropsch reaction for the synthesis of liquid hydrocarbons,[30-31] and for this reason the adsorption of hydrogen on Co surfaces has been investigated.[32-37] Several groups have studied the reactions of cobalt clusters with molecular hydrogen[38] and molecular deuterium.[39-41] From the theoretical side, the adsorption of atomic hydrogen on small cobalt clusters has been studied in using density functional theory.[42-45] Jones et al.[43] investigated the adsorption of one and two H atoms on small Co_n clusters with n= 1-4, focusing on the effect that H adsorption has on the magnetic moment of the cluster. Buendía and Beltrán[45] extended that work, investigating the adsorption of up to five H atoms on Co_n with n= 1-5. Nakhaei Pour et al.[42] enlarged the cluster size by considering several clusters between Co_4 and Co_{24}, but only one H atom was adsorbed in each case. Franczak et al.[44] studied the adsorption oh H and H^+ on several Co clusters with specific geometries modeling surfaces of the solid metal. The cited works have not investigated the saturation limit for hydrogen adsorption. In this paper we study the interaction of hydrogen with two cobalt clusters, Co_6 and Co_{13}. First, the molecular and dissociative adsorption of one and two hydrogen molecules is presented. Geometries, adsorption energies, electronic charge redistribution on adsorption, and the spin magnetic moments are discussed as well as the effect of the cluster size. After that, adsorption of additional hydrogen is investigated for the case of the smaller cluster, Co_6, and the competition between molecular and dissociative adsorption is analyzed as the number of added H_2 molecules increases. Saturation is obtained with 16 H_2 molecules. In this saturation limit the weight per cent of hydrogen on the cluster is 8.4 per cent, a promising result for the purposes of hydrogen storage.

B Theoretical model

Hydrogen adsorption and dissociation on two Co clusters, Co_6 and Co_{13}, is investigated using the Density Functional Formalism (DFT). The supercell methodology is used for the calculations, as implemented in the Dacapo code.[46] The cell is cubic, with a length side of 15 Å for Co_6 and 16 Å for Co_{13}, large enough to avoid interactions between image clusters in different cells. The energy of the isolated hydrogen molecule used as reference to obtain the hydrogen adsorption and dissociation energies on the cobalt clusters (see below

equations 1—3, 5) has been calculated using a cubic cell with 15 Å and 16 Å of side, for adsorption on Co_6 and Co_{13}, respectively. The Co atom has an electronic configuration $[Ar]4s^23d^7$, where [Ar] represents the argon-like core, which is replaced in the calculations by a pseudopotential. The calculations have been performed using (i) Vanderbilt ultrasoft pseudopotentials,[47] (ii) the generalized gradient approximation of Perdew and Wang (GGA-PW91)[48] for the exchange-correlation functional, (iii) a basis set of plane waves with cutoffs of 500 eV and 1000 eV for the expansion of the wave functions and the electronic density, respectively, and (iv) a grid of 2x2x1 k points selected in the first Brillouin zone following the Monkhorst-Pack scheme.[49] All the calculations allowed for spin polarization. An extensive search of the lowest energy configuration of the Co clusters and of the adsorbed hydrogen molecules and hydrogen atoms on the Co clusters has been performed. All the structures have been fully optimized till the forces on all the atoms were smaller than 0.05 eV/Å and the cohesive energies were converged within 10 meV.

C Clean Co_6 and Co_{13} clusters

The calculated structure of free Co_6, shown in Fig. 1, is an octahedron showing a very small distortion, in agreement with previous works.[23-25, 42] The Co-Co bond distances vary between 2.26 Å and 2.27 Å, the binding energy per atom is E_b = 3.03 eV, and the spin magnetic moment is μ = 14 $μ_B$ (2.33 $μ_B$ per atom).
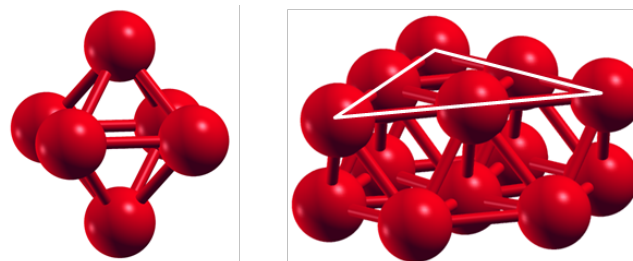

Figure 1. Ground state structures of Co_6 (octahedron), and Co_{13} (fcc fragment) in an orientation allowing the identification of the two parallel (1,1,1) Co planes, the upper plane being a triangle formed by six atoms (a white triangle joining the six atoms has been drawn to help visualization) and the bottom plane with seven atoms forming a hexagon with an atom at its center

A comparison with previous works is presented in Table 1. Those works used exchange-correlation energy functionals different from the PW91 used by us. Ma et al.[23] and Sebetci[25] used the BLYP functional,[50-51] Datta et al.[24] used the PBE functional,[52] and Nakhaei Pour et al.[42] used a revised PBE functional. There is full agreement for the magnetic moment between the different calculations. Our bonding distances agree with those calculated by Datta et al.[24] and Sebetci,[25] while Ma et al.[23] obtained larger interatomic distances, and Nakhaei Pour et al.[42] calculated bonding distances too small compared to all the other calculations. The binding energy shows substantial differences between the different calculations; our result is in reasonable agreement with that of

Datta et al.[24] We have also found a low lying structure of Co$_6$, an incomplete pentagonal bipyramid, with a binding energy per atom E_b = 2.85 eV. This configuration is similar to that of the lowest lying isomer of Pd$_6$.[55]

Table 1. Binding energy per atom E_b, distances d between nearest neighbor Co atoms and magnetic moment μ of Co$_6$ and Co$_{13}$. A comparison with experiment and with works using other exchange-correlation functionals is presented.

	Co$_6$			Co$_{13}$		
	E_b(eV/at)	d (Å)	μ (μ_B/at)	E_b(eV/at)	d (Å)	μ (μ_B/at)
This work (PW)	3.03	2.26-2.27	2.33	3.47	2.30-2.40	2.08
Ma (BLYP)[23]	3.57	2.38-2.40	2.33	3.85	-	1.77
Sebetci (BLYP)[25]	1.71	2.26-2.34	2.33	-	-	
Datta (PBE)[24]	2.92	2.27	2.33	3.28	-	1.92
Nakhaei (revPBE)[42]	1.98	1.77		2.56	2.51	
experimental						2.30[a];2.00[b,c]

(a) Knickelbein;[53] (b) Xu et al.;[54] (c) Datta et al.[24]

The ground state structure of Co$_{13}$ is an fcc fragment formed by two parallel (111) fcc planes. The structure is shown in Fig. 1, in an orientation allowing the identification of the two Co planes. The upper plane has six atoms forming a triangle, and the bottom plane is a hexagon with an atom on its center. The structure is similar to that found in Pd$_{13}$.[20] The distances between neighbor Co atoms vary between 2.30 Å y 2.40 Å, the binding energy is 3.47 eV per atom, and the magnetic moment is μ = 27 μ_B (2.08 μ_B per atom). Co$_{13}$ has two low-lying isomers, icosahedron and cuboctahedron, both with E_b = 3.33 eV/atom, a bit lower than that of the ground state. The increase of the interatomic distances and binding energy between Co$_6$ and Co$_{13}$, and the decrease of the magnetic moment, are consistent with the expectations for the variation of those properties with the number of atoms in the clusters.[3] Previous works, using other exchange-correlation energy functionals, have found different structures for Co$_{13}$. Ma et al.[23] obtained a distorted icosahedron with E_b = 3.85 eV/atom and μ = 1.77 μ_B/atom. Nakhaei Pour et al.[41] found a structure that in the published figure looks like a hexagonal close packed structure formed by a hexagonal ring with an atom at the center, and two triangular planes above and below the hexagonal ring, respectively, giving a 3,7,3 stacking. This structure, with E_b = 2.56 eV/atom, is related to our structure in Fig. 1; it is obtained by moving three Co atoms from the triangular face to the other side of the hexagonal plane. Datta et al.[24] obtained a heavily distorted version of the hexagonal structure mentioned above, with E_b = 3.28 eV/atom and μ = 1.92 μ_B/atom). Again we find good agreement between our binding energy and the result of Datta et al. The magnetic moment of Co$_{13}$ has been measured, and our calculated spin moment lies in between the two experimental values. In spite of the differences in the predicted structures of Co$_{13}$, all the Co$_{13}$ structures mentioned above are quite compact and we do not expect significant changes in their capacity to adsorb hydrogen. On the other hand, our calculation delivers spin magnetic moments in agreement with experiment for Co$_{13}$, and in agreement with other calculations for Co$_6$.
A plot of the distribution of spin polarization in the cluster, $\Delta\rho_{spin}(\vec{r})$ = $\rho_{up}(\vec{r})$-$\rho_{down}(\vec{r})$, where $\rho_{up}(\vec{r})$ and $\rho_{down}(\vec{r})$ are the density of electrons with up and down spin orientation, respectively, reveals (see Fig. 2) that there is an excess of up spin (the majority spin) around the Co atoms and in the outer part of the cluster, while the inner part and the regions between Co atoms have an excess of down spin (the minority spin). Figure 2 also shows the redistribution of the electronic density on Co$_n$ (n=6, 13), $\Delta\rho(\vec{r})$ = ρ[Co$_n$]-n ρ[Co], that is, the difference between the electronic density of Co$_n$ minus the superposition of the electronic densities of n isolated Co atoms placed on their final positions in Co$_n$. There is an enhancement of electron density in the region between de atoms and a small depletion of electronic density from the outer part of the cluster what reflects a kind of metallic type of bonding between the Co atoms in the cluster. It is interesting to notice that the enhancement of electronic density correlates with the regions with an excess of down spin density. This indicates that it is the redistribution of the spin down electrons what leads to the bonding of the cluster.
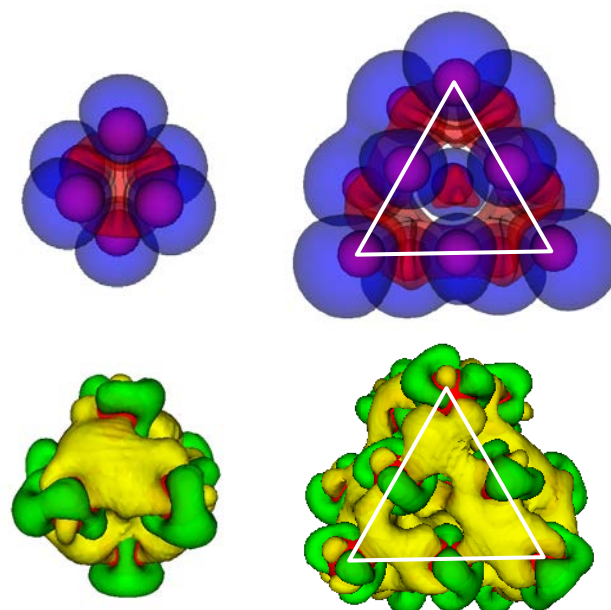
Figure 2. Upper figures show the spatial distribution of spin polarization in the cluster, $\Delta\rho_{spin}(\vec{r})$ = $\rho_{up}(\vec{r})$ - $\rho_{down}(\vec{r})$, where $\rho_{up}(\vec{r})$ and $\rho_{down}(\vec{r})$ are the density of electrons with up and down spin orientation, respectively. Co$_6$, left, and Co$_{13}$, right; a white triangle joining the six atoms of the upper layer of Co$_{13}$ has been drawn to help visualization. Blue and red colors mark surfaces with $\Delta\rho_{spin}$= +0.02 e/Å^3 and -0.02 e/Å^3, respectively. Lower figures show the electronic density redistribution, $\Delta\rho(\vec{r})$=ρ[Co$_n$]–n ρ[Co],where ρ[Co$_n$] is the total electronic density of Co$_n$ from which it is subtracted the densities of the n Co atoms, ρ[Co], taken in their final positions in Co$_n$. Co$_6$, left, and Co$_{13}$, right. Yellow and green colors indicate regions where the electron density increases and decreases, respectively. The plotted surfaces have values +0.05 e/Å^3 and -0.05 e/Å^3, respectively.

D Adsorption of H_2 at low coverage on Co_6: one and two hydrogen molecules

The most stable adsorption configuration of H_2 on Co_6 occurs for the H_2 molecule adsorbed on top of a Co atom. This configuration is shown in the bottom panel of Fig. 3, but there are other nearly equivalent adsorption positions due to the symmetry of the cluster. The H-H bond distance of the adsorbed molecule, d(H-H) = 0.800 Å, is slightly larger than the bond length d(H-H) = 0.754 Å in free H_2 (experimental d(H-H) = 0.76 Å). This indicates that the H_2 molecule becomes a little activated upon adsorption. The molecular adsorption energy

$$E_{mol} = E(Co_6) + E(H_2) - E(H_2@Co_6) \qquad (1)$$

where $E(Co_6)$, $E(H_2)$ and $E(H_2@Co_6)$ are the total energies of the clean Co cluster, the molecule, and the combined system formed by the molecule adsorbed on the cluster, respectively, amounts to 0.120 eV. H_2 adsorption does not change the spin magnetic moment from its value μ (Co_6) = 14 μ_B for the clean cluster. Moreover, the spatial distribution of the spin density polarization (see Fig. 3) is almost identical to that of the clean Co_6 cluster, and the region around the H_2 molecule is nearly spin compensated. A second H_2 molecule can be adsorbed on top of any of the other five Co atoms. The most stable configuration corresponds to adsorption on a Co atom opposite (non-adjacent) to the one hosting the first molecule. The adsorption energy of the second molecule

$$E_{mol}(second) = E(H_2@Co_6) + E(H_2) - E(2H_2@Co_6) \qquad (2)$$

is 0.554 eV, a value higher than that of the first molecule. This indicates that the Co_6 cluster with one preadsorbed H_2 molecule is more reactive than the clean cluster (a similar behavior is observed for the dissociative adsorption of H_2, and for hydrogen adsorption on Co_{13}; see below). The spin magnetic moment changes to $\mu(2H_2@Co_6)$ = 12 μ_B. The H-H bond distances of the two adsorbed molecules are equal, d(H-H) = 0.868 Å. On the other hand, adsorption of the second H_2 molecule on a neighbor Co atom leads to a lower adsorption energy, 0.13 eV, and the system has spin magnetic moment μ = 14 μ_B.

Simulations starting with one H_2 molecule on top of faces or edges of the octahedron end up in dissociated states of the molecule. Different possibilities exist for the location of the two H atoms on top of faces and edges of the octahedron. The chemisorption energy in the dissociative configuration is defined

$$E_{diss} = E(Co_6) + E(H_2) - E(2H@Co_6), \qquad (3)$$

where $E(2H@Co_6)$ is the energy of the system formed by two separated H atoms chemisorbed on the cluster, and the other energies have the same meaning as before. In other papers, the isolated free atoms are used sometimes as the reference, instead of the H_2 molecule. Here we prefer using the free molecule, because it is the natural reference when one is
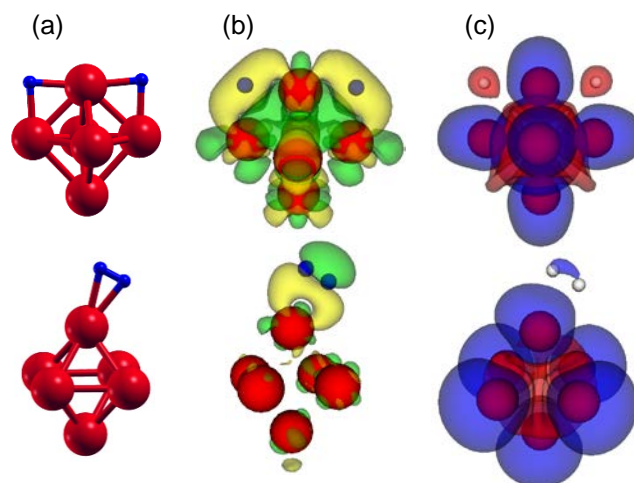

Figure 3. Top panels show: (a) Lowest energy structure of Co_6 with two chemisorbed H atoms. Large and small spheres represent Co and H atoms, respectively. (b) Electron density redistribution after chemisorption of two H atoms (see text). Yellow and green colors indicate regions where the electron density increases and decreases, respectively. The plotted surfaces have values $\Delta\rho(\vec{r})$ = +0.01 e/Å^3 and -0.01 e/Å^3, respectively. (c) Spatial distribution of spin density polarization. Blue and red colors mark regions of positive and negative values of the spin density polarization. The plotted surfaces have values $\Delta\rho_{spin}(\vec{r})$ = +0.02 e/Å^3 and -0.02 e/Å^3, respectively. The bottom panels show the structure, $\Delta\rho(\vec{r})$ and $\Delta\rho_{spin}(\vec{r})$, respectively, for molecular H_2 adsorbed on Co_6.

interested in the process of pumping hydrogen into a container like a porous material, or into a fuel cell. The dissociative adsorption energies with the H atoms on top of faces of the octahedron vary between 0.25 eV and 0.35 eV, and the adsorption energies with the H atoms on top of edges are higher than 0.40 eV. Those values are in all cases larger than the energy for molecular adsorption, 0.12 eV. The most stable dissociated configuration is shown in the upper panel of Fig. 3. The two H atoms are attached to the cluster in bridge positions on top of two non-adjacent edges. The Co-H bond distances are all equal to 1.68 Å, and the adsorption energy is E_{diss} = 0.60 eV. A plot of the redistribution of the electronic density

$$\Delta\rho(\vec{r}) = \rho(2H@Co_6) - \rho(Co_6) - 2\rho(H), \qquad (4)$$

that is, the electron density of the final system, $2H@Co_6$, minus the densities of the individual isolated fragments, Co_6 and two H atoms in their final positions in $2H@Co_6$, reveals (see Fig. 3) an enhancement of the electron density in the neighborhood of the H atoms, at the expense of a loss of charge by the Co atoms. There is, then, a kind of ionic bonding, like in metallic hydrides. In contrast, the electronic redistribution after adsorption of molecular hydrogen (see the bottom panel of Figure 3) shows a weak covalent type of bonding between H_2 and the Co cluster with substantial polarization of the charge of the molecule. It is interesting to notice that the preferred adsorption site of H_2, on top of a Co atom, correlates with the regions of electron density depletion of the Co_6 cluster (see Fig.2). The H_2 molecule has a closed shell structure and its adsorption on the cluster leads to a

substantial polarization of the electron density. In contrast, the adsorption sites of H atoms, bridge positions, correlate with regions with enhanced electron density (see Fig.2). The H atom acquires electronic charge from the Co cluster what leads to an ionic type of bonding.

The total spin magnetic moment has dropped from the value $\mu(Co_6) = 14 \mu_B$ of the clean cluster to $\mu(2H@Co_6) = 12 \mu_B$. As a consequence, the spatial distribution of spin polarization (see Fig. 3) is more concentrated around the Co atoms than in the clean Co_6 cluster, and the regions around the two H atoms have a small excess of the minority spin charge. The drop in the magnetic moment can be understood from the density of electronic states (DOS). DOS, separated in spin up and spin down components, are shown in Fig. 4 for pristine Co_6 and $2H@Co_6$. The peaks corresponding to the one-electron energies have been broadened by Lorentzian functions. The DOS of pristine Co_6 exhibits two deep electronic levels (with spin up and spin down character, respectively) at about -6 eV, and two broad bands, one band above -4.5 eV for the spin up states and the other above -3.0 eV for the spin down states. The DOS of spin down electrons (minority electrons) is shifted with respect to that of spin up electrons (majority electrons), and this gives rise to the high magnetic moment of the cluster, 14 μ_B. The energy gap between occupied and unoccupied sates for majority electrons, Δ_{up} (Co_6) = 2.45 eV, is substantially larger than the gap for minority electrons, Δ_{down} (Co_6) = 0.62
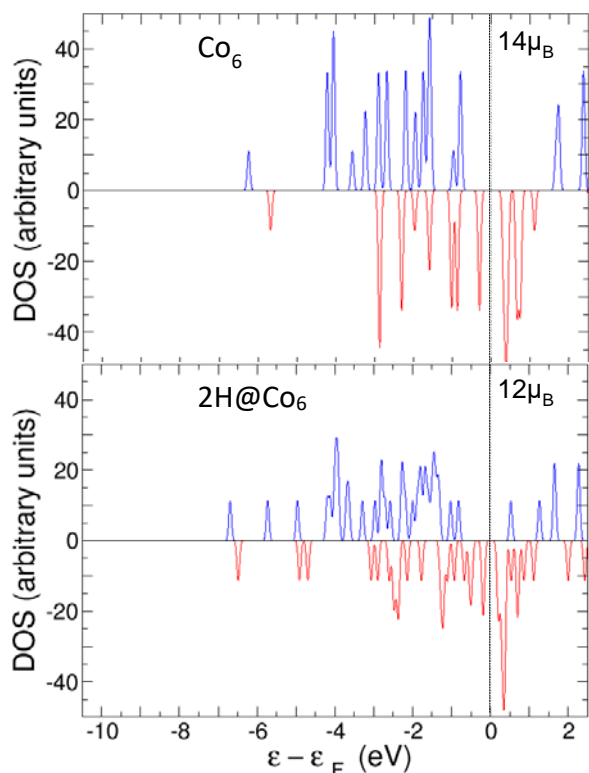
eV. In the case of dissociative adsorption of a single hydrogen molecule, which corresponds to the panel labelled 2H, new states with hydrogen character appear, one with spin up and one with spin down per hydrogen atom. These four states have binding energies in the range -6.0 to -4.5 eV, and hybridize with the deepest levels of the Co_6 cluster. One can interpret that the two hydrogen-like states with spin up are occupied by the electrons contributed by the H atoms. On the other hand, the two hydrogen states with spin down result from a transfer from the spin up Co band near the Fermi level to the spin down group, plus further energy stabilization. In fact, a lowering of the height and width of some spin up peaks below the Fermi level is appreciated by comparing the Co_6 and 2H panels. This change of spin orientation, from up spin to down spin, is responsible for the drop in the magnetic moment in the $2H@Co_6$ cluster. The filling of the spin down state on each H atom becomes reflected in the charge accumulation around the H positions shown in the upper panel of Fig. 3.

The minimum energy configuration of Co_6 with two adsorbed molecules is given in Fig. 5. In this configuration, the two hydrogen molecules are dissociated, and the four H atoms occupy bridge positions on top of edges of the octahedron, two H atoms on the upper half of the octahedron and two H atoms on the lower half. The spin magnetic moment is $\mu(4H@Co_6)$ = 12 μ_B, with no change with respect to $\mu(2H@Co_6)$. The chemisorption energy of the second dissociated molecule, defined

$$E_{diss} \text{ (second)} = E(2H@Co_6) + E(H_2) - E(4H@Co_6), \quad (5)$$

is E_{diss}(second) = 1.42 eV, substantially larger than the chemisorption energy of the first dissociated molecule. The most likely reason is that the structure of $4H@Co_6$ is quite symmetric, the four H atoms forming a plane with four Co atoms. The six Co atoms can be viewed as forming two groups. The first group includes four Co atoms forming a common plane with the four H atoms. Each of those Co atoms is bonded to two H atoms. The second group includes the remaining two

Figure 5. (a) Lowest energy structure of Co_6 with two dissociated molecules (four chemisorbed H atoms). (b) Electron density redistribution after chemisorption of four H atoms. Yellow and green colors indicate regions where the electron density increases and decreases, respectively. The values of the density difference isosurfaces are the same as in Fig.3.
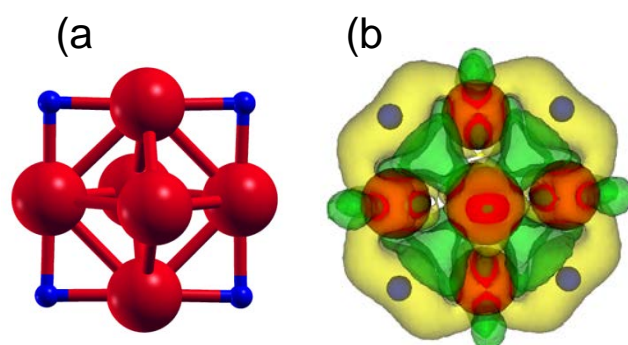

Figure 4. Density of electronic states (DOS) of Co_6 (upper panel) and Co_6 with a dissociated molecule adsorbed, $2H@Co_6$ (lower panel). The DOS is separated in spin up (blue) and spin down (red) components. The Fermi level, at energy = 0 is indicated by a thin vertical line. The magnetic moments are given in each panel.

Co atoms, not bonded to H atoms. The electron density redistribution (with respect to Co_6 and four H atoms), shown in Fig. 5(b), is consistent with that in $2H@Co_6$ (upper panel of Fig. 3). Other isomeric structures exist for $4H@Co_6$, with different arrangements of the four H atoms over the edges of the octahedron, but those arrangements have lower adsorption energies.

E Adsorption of H_2 at low coverage on Co_{13}: one and two hydrogen molecules

An H_2 molecule can be adsorbed on Co atoms of the vertices and edges of the two parallel layers forming the fcc-like structure of Co_{13} with adsorption energies ranging between 0.22 and 0.45 eV. The most stable configuration of the adsorbed molecule is shown in Fig. 6. The molecule is attached to a Co atom placed on the edge of the triangular six-atom planar face of the cluster. The molecular adsorption energy is 0.45 eV.
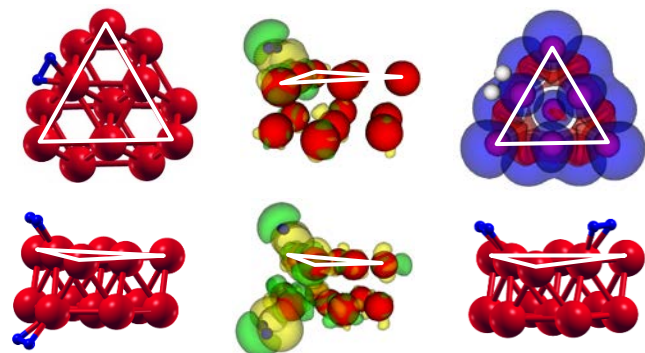

Figure 6. Upper row: Lowest energy configuration for an H_2 molecule adsorbed on Co_{13}, electron density redistribution on H_2 adsorption, and spin density. Lower row: Lowest energy configuration for two H_2 molecules adsorbed on Co_{13} and electron density redistribution after the adsorption of the two H_2 molecules. The right panel shows other isomeric configuration of $2H_2@Co_{13}$. In both $2H_2@Co_{13}$ structures one of the H_2 molecules is in the same position as in $H_2@Co_{13}$. A white triangle joining the six atoms of the upper face of the cluster has been drawn to help visualization. The color code and the values of the density difference and the spin density isosurfaces are the same as in Fig.3.

The electronic redistribution on H_2 adsorption shows that the electronic charge of the molecule becomes spatially polarized (central panel of the upper row of Fig. 6) and this is consistent with the redistribution found in $H_2@Co_6$ (Fig. 3). On the other hand, there is no change in the spin polarization of the cluster after adsorption of the molecule, and this can be appreciated in a comparison of the spin density plots of free Co_{13} (Fig. 2) and $H_2@Co_6$ (Fig. 6). Thus, the magnetic moment keeps the value $\mu = 27\ \mu_B$ of clean Co_{13}. Notice that the region about the adsorbed hydrogen molecule is perfectly spin compensated.

Starting with the most stable structure of $H_2@Co_{13}$, a search for the preferred configuration for a second adsorbed molecule delivers a number of allowed structures. The second H_2 molecule can be attached to any of the clean Co atoms of

the cluster. The most stable configurations are shown in Fig. 6, and the two H_2 molecules sit on neighbor Co atoms. In the structure shown on the left panel, the second H_2 molecule is attached to a Co atom of the bottom (seven atom) planar face, while in the structure show on the right panel the second molecule is attached to a Co atom of the upper (six-atom) planar face. The adsorption energies of the second molecule are very similar: 0.47 eV and 0.42 eV, respectively. The spin magnetic moment of the lowest energy structure drops to $\mu = 25\ \mu_B$.
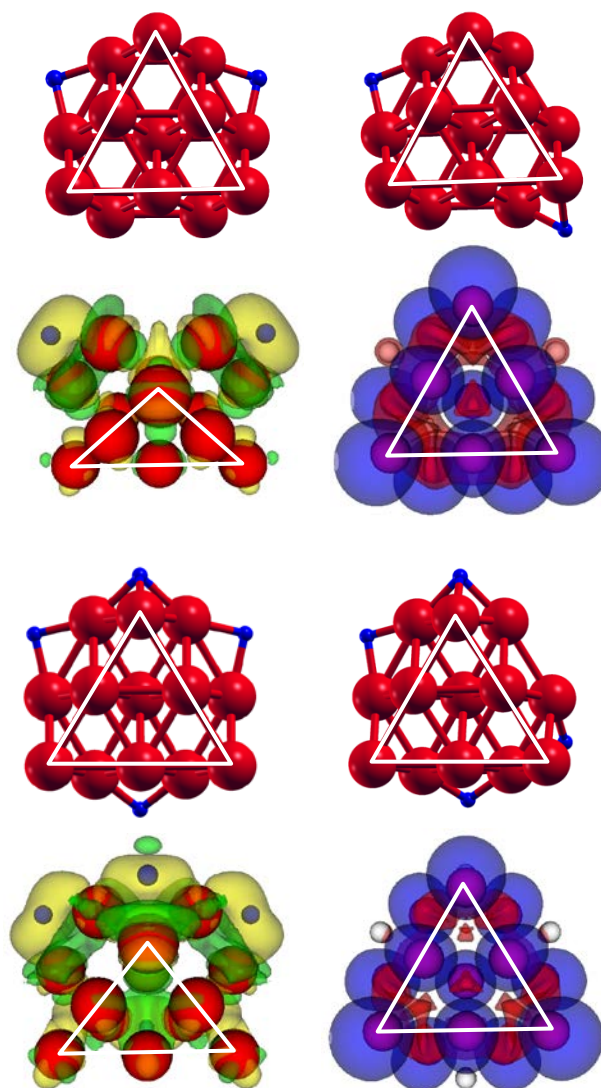
Figure 7. Structures of two isomeric dissociated chemisorption configurations for $2H@Co_{13}$ (first row) and $4H@Co_{13}$ (third row). The configurations on the left are those with the highest chemisorption energies. Second and forth rows show the electron density redistribution after the adsorption of hydrogen (left) and the spin density (right) of the lowest energy configurations of $2H@Co_{13}$ and $4H@Co_{13}$, respectively. A white triangle joining the six atoms of the upper face of the cluster has been drawn to help visualization. The color code and the values of the density difference and the spin density isosurfaces are the same as in Fig.3.

However, configurations with the molecules dissociated and the H atoms occupying different positions on top of edges or faces of Co_{13} are more stable than the molecular configuration. Two selected dissociated configurations for a single adsorbed molecule are shown on the upper row of Fig. 7. The one of the left panel is the configuration with the highest adsorption energy, 1.47 eV. In that structure, the two H atoms are on bridge positions between Co atoms forming the border of the seven-atom plane. In the structure of the right panel, one of the H atoms also occupies a bridge position between Co atoms forming the border of the bottom (seven-atom) plane, whereas the second H atom occupies a bridge position between a border atom of the bottom plane and a corner atom of the six-atom plane. The adsorption energy in this configuration is smaller, 1.14 eV. The adsorption energies in the molecular and dissociated configurations on Co_{13} are larger than the corresponding adsorption energies on Co_6. Interatomic H-Co distances, on the other hand, have the same value, 1.68 Å, found in the case of Co_6. The electron density

redistribution and the spin polarization corresponding to the lowest energy structure of 2H@Co_{13} are shown in the second row of Fig. 7. The accumulation of electronic charge observed near the H atoms was already noticed for dissociative adsorption on Co_6 (see Fig. 3). The magnetic moment drops from the value μ = 27 μ_B of clean Co_{13} to μ = 25 μ_B on 2H@Co_{13}. This is reflected in a slight reduction of the spin polarization at the H adsorption sites (compare Figs. 2 and 7). In the case of two dissociated molecules, the H atoms tend to be not close together. The two configurations shown in the third row of Fig. 7 have total adsorption energies of 2.87 (left panel) and 2.48 eV (right panel). Consequently, the average adsorption energies per molecule are 1.44 and 1.24 eV, respectively, close to the dissociative adsorption energies of a single molecule in the two configurations on the upper row of Fig. 7. The spin magnetic moment of these 4H@Co_{13} clusters is μ = 25 μ_B.
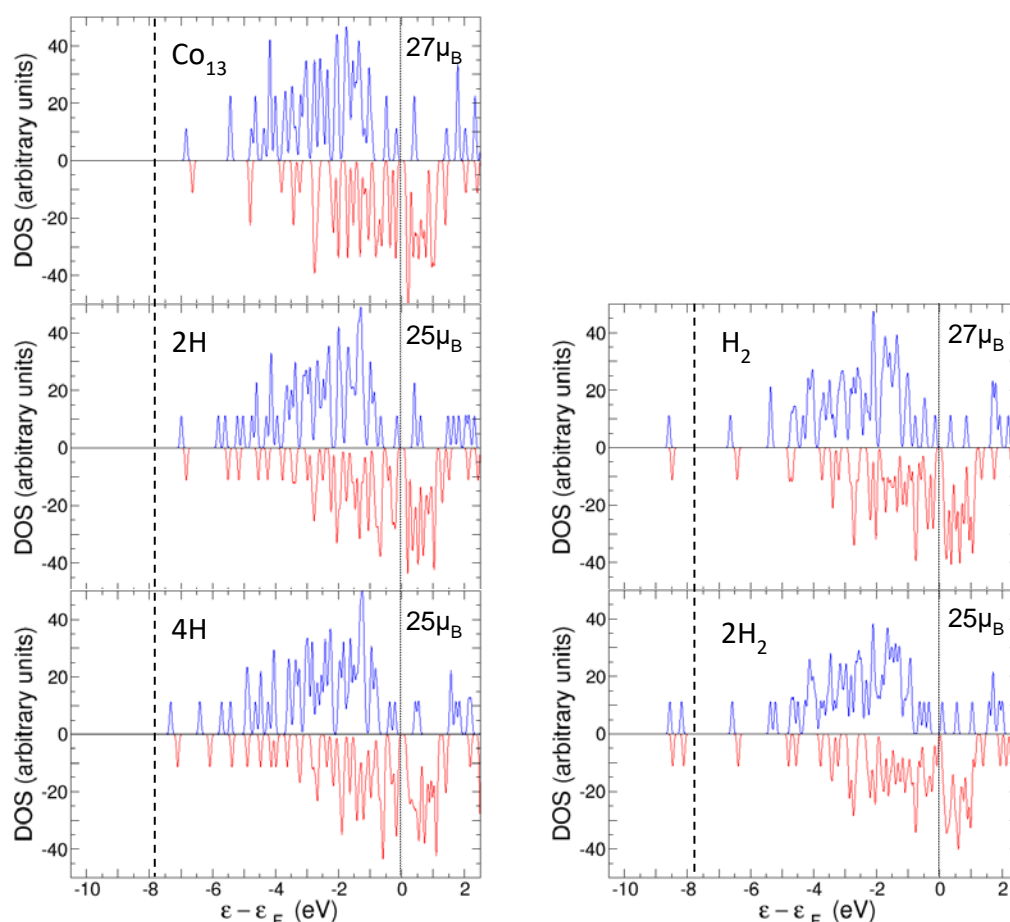
Fig. 8. The different panels give the DOS of Co_6, Co_6 with one and two dissociated adsorbed molecules (panels labelled 2H and 4H, in the left column) and Co_6 with one and two non-dissociated adsorbed molecules (panels labelled H₂ and 2H₂ in the right column). The DOS is separated in spin up (blue) and spin down (red) components. The Fermi level, at energy = 0, is indicated by a thin vertical black line. The thick vertical line helps to identify the deep levels associated to the non-dissociated H₂ molecules (peaks on the left of that line). The magnetic moments are given in each panel.

The magnetic moments and the different type of bonding of molecular and dissociated hydrogen adsorbed on Co_{13} are reflected in the DOS plots of Fig. 8. This Figure shows the DOS of pristine Co_{13}, Co_{13} with one and two non-dissociated adsorbed molecules (panels H_2 and $2H_2$ on the right column), and Co_{13} with one and two dissociated molecules (panels 2H and 4H on the left column). Similar to Co_6, the DOS of pristine Co_{13} shows two deep levels, one with spin up and one with spin down, between -7.0 eV and -6.5 eV, and a broad band above -5.5 eV and -4.7 eV for spin up and spin down, respectively. Each non-dissociated H_2 molecule adsorbed on Co_{13} introduces two very deep levels (one with spin up and one with spin down character) in the DOS, deeper than all the electronic states of Co_{13}. Those deep levels are the peaks on the left side of the thick vertical line in the panels H_2 and $2H_2$ of Fig. 8. Those two levels (per H_2 molecule) are populated by the two electrons contributed by the hydrogen molecule and do not hybridize with the levels of the Co cluster, resulting in small adsorption energies (less than 0.5 eV) for molecular hydrogen. This is in contrast with dissociative adsorption on Co_{13}. The panels 2H and 4H show that each H atom of the dissociated molecule introduces two electronic levels (one with spin up and one with spin down) in the deep region (between -8 and -4 eV) of the Co band, but contributes with only one electron to the system. Thus one can interpret that the two levels with spin up are filled by the electrons provided by the hydrogen atoms and the two levels with spin down are filled with electrons transferred from spin up Co states near the Fermi level. The levels introduced by atomic hydrogen exhibit a substantial hybridization with the deepest energy levels of Co_{13}, leading to the stabilization of the system and to higher adsorption energies than molecular adsorption. A similar behavior has been found for dissociative hydrogen adsorption on Co_6 as explained above.

A comparison of the adsorption energies of one and two H_2 molecules (dissociated and not dissociated) on Co_6 and Co_{13}, given in Table 2, indicates that the bonding of hydrogen to the cluster is stronger on Co_{13}. This can be rationalized by considering the magnitude of the gap between the highest occupied molecular orbital (HOMO) and the lowest unoccupied molecular orbital (LUMO) of the bare Co clusters. The HOMO-LUMO gap Δ gives a measure of the reactivity (or the chemical hardness) of a cluster.[56, 57] The gaps of the spin up channel, Δ_{up} (Co_6) = 2.45 eV, and spin down channel, Δ_{down} (Co_6) = 0.62 eV, in Co_6 are larger than the corresponding gaps in Co_{13}, Δ_{up} (Co_{13}) = 0.57 eV, Δ_{down} (Co_{13}) = 0.36 eV (the gap between the $HOMO_{up}$ and the $LUMO_{down}$ in Co_{13} is 0.45 eV), a feature which supports the higher reactivity of Co_{13}, and consequently explains the enhanced adsorption energy of hydrogen in Co_{13}. A similar relation between the magnitude of the gaps, namely $\Delta(Co_6) > \Delta(Co_{13})$, was obtained by Ma et al.[23]

F Saturation of Co_6 with hydrogen

The sequential addition of more hydrogen, until reaching saturation, has been studied in the case of the smaller cluster, Co_6. Starting with 4H@Co_6, addition of the third and fourth H_2 molecules leads to dissociative adsorption, 6H@Co_6 and 8H@Co_6 structures (see Fig. 9), with the H atoms in bridge positions between Co atoms. The four H atoms added to 4H@Co_6 to form 8H@Co_6 lie on a plane perpendicular to the plane of the four H atoms in 4H@Co_6. The chemisorption energies of the third and fourth dissociated molecules are 0.28 and 1.02 eV, and the magnetic moments are μ(6H@Co_6) = $12\mu_B$, and μ(8H@Co_6) = $10\mu_B$. The structure of 8H@Co_6 is more symmetric than that of 6H@Co_6, and this is the reason for the higher adsorption energy of the last dissociated molecule in 8H@Co_6. The Co atoms in 6H@Co_6 can be separated in three groups of two Co atoms each: the Co atoms of the first group form bonds with three H atoms, the Co atoms of the second group form bonds with two H atoms, and the Co atoms of the third group form one Co-H bond. In 8H@Co_6, two Co atoms are bonded, each one, to four H atoms, and four Co atoms are bonded to two H atoms each. It is noticeable that the dissociative chemisorption of eight H atoms preserves the geometrical structure of the Co_6 cluster.
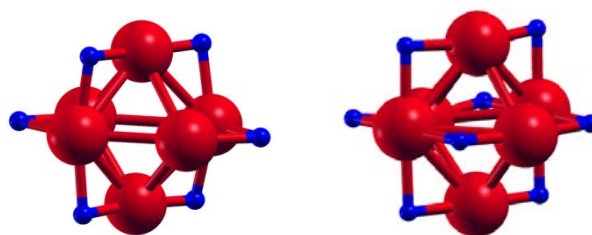

Fig. 9. Lowest energy structures of Co_6 with six and eight chemisorbed H atoms.

An interesting change occurs when adding the fifth H_2 molecule. The cluster is unable to dissociate that molecule, but is able to adsorb it in molecular form on top of a Co atom, as shown in Fig. 10. That particular host atom is one of the Co atoms coordinated to only two H atoms in 8H@Co_6. The structure of the cluster is then described as (8H+H_2)@Co_6. Additional hydrogen molecules can then be adsorbed on top of the other five Co atoms, one molecule on each Co, until reaching (8H+6H2)@Co_6. Fig. 10 shows the structures of (8H+2H_2)@Co_6 and (8H+6H_2)@Co_6. The successive adsorption energies of the last molecule in this family are given in Table 2. The trend in the adsorption energies is better displayed in Fig. 11, which reveals a decrease of the adsorption energies E_{mol} and E_{diss} as the coverage increases. However this decrease is non smooth; instead, it displays sizable oscillations, especially at the beginning. Interestingly, the spin magnetic moment does not vary between (8H+H_2)@Co_6 and (8H+6H_2)@Co_6, remaining at the value μ =$10\mu_B$. The electron density redistribution following molecular H_2 adsorption is very different from the density redistribution associated to dissociative chemisorption discussed above. Fig. 10 shows an

Table 2. Number of molecules added to Co_6 and Co_{13}, structure of the cluster with adsorbed hydrogen (nH indicates n chemisorbed hydrogen atoms, and mH_2 indicates m adsorbed hydrogen molecules), adsorption energy of the last adsorbed molecule (dissociated or in molecular form), average adsorption energy per molecule and spin magnetic moment. The lowest energy channel for adsorption of hydrogen and the adsorption following the molecular channel are shown separately. See text for details.

H_2 molecules	structure	$E_{mol/diss}$(last) (eV)	E_{ads}(average) (eV/molecule)	mag. moment (μ_B)
0	Co_6	-	-	14
	Lowest energy channel			
1 H_2	$2H@Co_6$	0.60	0.60	12
2 H_2	$4H@Co_6$	1.42	1.01	12
3 H_2	$6H@Co_6$	0.28	0.77	12
4 H_2	$8H@Co_6$	1.02	0.83	10
5 H_2	$(8H+H_2)@Co_6$	0.43	0.75	10
6 H_2	$(8H+2H_2)@Co_6$	0.57	0.72	10
7 H_2	$(8H+3H_2)@Co_6$	0.71	0.72	10
8 H_2	$(8H+4H_2)@Co_6$	0.40	0.68	10
9 H_2	$(8H+5H_2)@Co_6$	0.53	0.66	10
10 H_2	$(8H+6H_2)@Co_6$	0.26	0.62	10
11 H_2	$(8H+7H_2)@Co_6$	0.38	0.60	6
12 H_2	$(8H+8H_2)@Co_6$	0.69	0.61	6
13 H_2	$(8H+9H_2)@Co_6$	0.25	0.58	4
14 H_2	$(8H+10H_2)@Co_6$	0.43	0.57	4
15 H_2	$(8H+11H_2)@Co_6$	0.19	0.54	2
16 H_2	$(8H+12H_2)@Co_6$	0.46	0.54	0
	Molecular channel			
1 H_2	$H_2@Co_6$	0.12	0.12	14
2 H_2	$2H_2@Co_6$	0.55	0.34	12
3 H_2	$3H_2@Co_6$	0.14	0.27	12
4 H_2	$4H_2@Co_6$	0.63	0.36	10
5 H_2	$5H_2@Co_6$	0.17	0.32	10
6 H_2	$6H_2@Co_6$	0.55	0.36	8
7 H_2	$7H_2@Co_6$	0.60	0.40	8
8 H_2	$8H_2@Co_6$	0.69	0.43	8
0	Co_{13}	-	-	27
	Lowest energy channel			
1 H_2	$2H@Co_{13}$	1.47	1.47	25
2 H_2	$4H@Co_{13}$	1.40	1.44	25
	Molecular channel			
1 H_2	$H_2@Co_{13}$	0.45	0.45	27
2 H_2	$2H_2@Co_{13}$	0.47	0.46	25
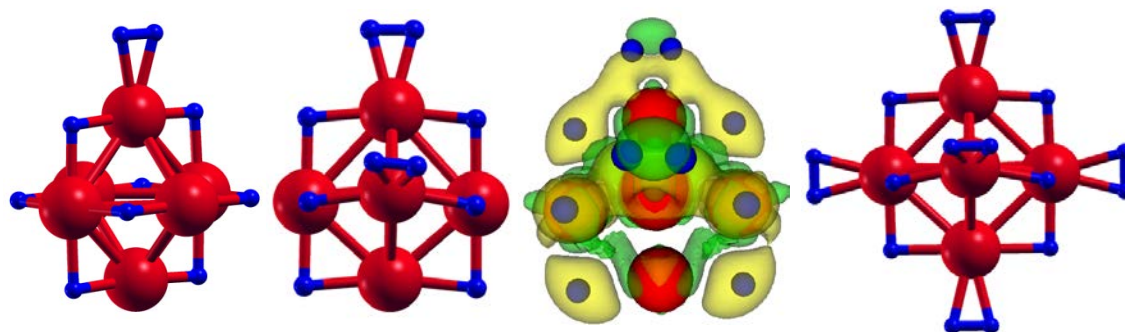
Fig. 10. Structure of $(8H+H_2)@Co_6$, $(8H+2H_2)@Co_6$ and $(8H+6H_2)@Co_6$; and electron density redistribution after adsorption of six H_2 molecules on Co_6, four of them dissociated. Yellow and green colors indicate regions where the electron density increases and decreases, respectively. The plotted surfaces have values $\Delta\rho(\vec{r}) = +0.04\ e/Å^3$ and $-0.04\ e/Å^3$, respectively.
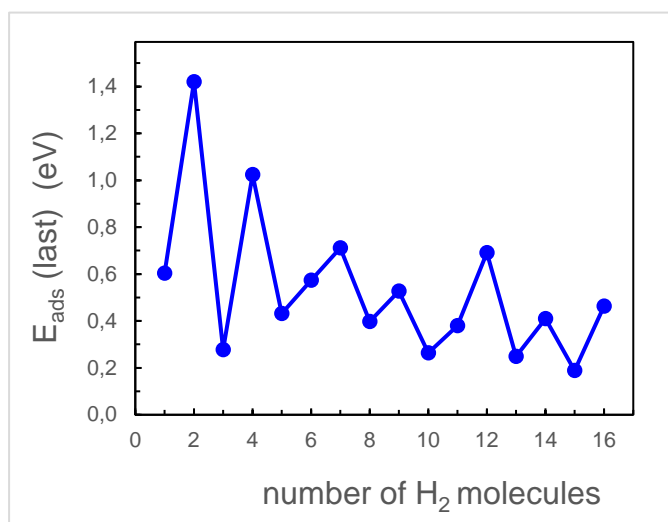

Figure 11. Adsorption energy of the last H_2 molecule as the coverage of the Co_6 cluster increases. Notice that the first four molecules are dissociated, and the rest are adsorbed in molecular form.

analysis for $(8H+2H_2)@Co_6$. The contours plotted correspond to

$$\Delta\rho(\vec{r}) = \rho((8H+2H_2)@Co_6) - \rho(Co_6) - 8\rho(H) - 2\rho(H_2), \quad (6)$$

that is, the electron density of the final system $(8H+2H_2)@Co_6$, minus the densities of the individual isolated fragments, Co_6, eight H atoms and two H_2 molecules in their final positions in the combined system. The figure allows for a comparison of dissociated chemisorption and molecular adsorption. There is an accumulation of electronic density around the eight dissociated H atoms, as discussed above; on the other hand, the charge of the two adsorbed molecules becomes

substantially polarized (green contours at one side and yellow contours at the other side).

At the composition $(8H+6H_2)@Co_6$, each one of the six Co atoms hosts a non-dissociated H_2 molecule. The adsorption energies of the non-dissociated H_2 molecules are still sizable (0.53 eV for the fifth molecule and 0.26 eV for the sixth molecule), and one may expect that the cluster adsorbs additional hydrogen by attaching a second molecule to the Co atoms (this occurs, for instance, in Pd clusters).[58] Indeed, it is possible to attach two non-dissociated molecules to each Co atom until reaching the limiting composition $(8H+12H_2)@Co_6$. The successive adsorption energies, given in Table 2, keep sizable values. This can also be appreciated in the average adsorption energies per molecule of Table 2,

$$E_{ads}(average) = E(Co_6) + E((m+n/2)H_2) - \frac{E((nH+mH_2)@Co_6)}{m+(n/2)}$$

$$(7)$$

n= 2, 4, 6, 8, m= 1-12. The average adsorption energy oscillates in the initial dissociative chemisorption regime, but after that it remains smooth, keeping a nearly constant value. Adsorption of the second non-dissociated H_2 molecule on the Co atoms affects the magnetic moment of the cluster, which decreases fast from a value $\mu = 10\ \mu_B$ for $(8H+6H_2)@Co_6$ to $\mu = 0$ at $(8H+12H_2)@Co_6$. The adsorption capacity of the cluster reaches saturation with 16 hydrogen molecules, four dissociated (with the eight H atoms on bridge positions on top of cluster edges) and 12 non-dissociated, two molecules on each Co atom of the cluster.
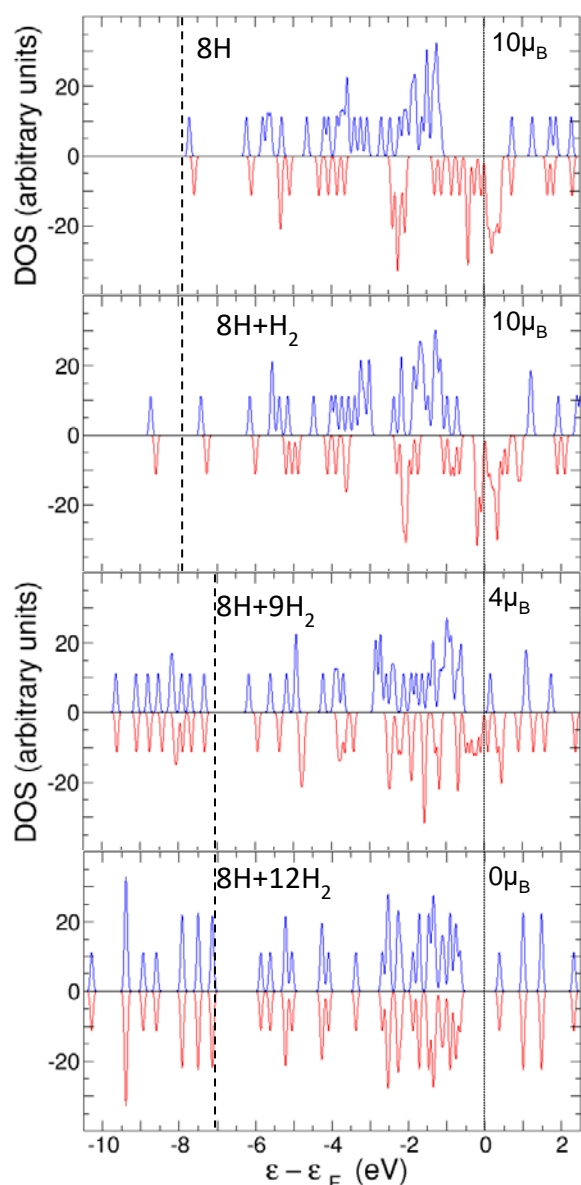
Figure 12. Density of electronic states (DOS) of Co_6 with increasing amounts of adsorbed hydrogen. Top panel, labelled 8H, corresponds to Co_6 with four dissociated molecules (8H atoms), and the other three panels stand for Co_6 with dissociated and non-dissociated molecules adsorbed at the same time. Labels $8H+H_2$, $8H+9H_2$ and $8H+12H_2$ represent adsorption of four dissociated molecules and m non-dissociated molecules, m = 1, 9, 12. The DOS is separated in spin up (blue) and spin down (red) components. The Fermi level, at energy = 0 is indicated by a thin vertical line. The thick vertical line in each panel separates the electronic levels originating from molecular H_2 (those at the left of the line) from the rest. The magnetic moments are given in each panel.

The DOS of the doped Co_6 clusters are shown in Fig. 12 as a function of increasing hydrogen coverage. Four cases are shown. The top panel, labelled 8H, corresponds to Co_6 with four dissociated molecules (8H atoms), and the other three panels stand for Co_6 with dissociated and non-dissociated molecules adsorbed at the same time. Labels $8H+H_2$, $8H+9H_2$ and $8H+12H_2$ represent the adsorption of four dissociated

molecules and m non-dissociated molecules (m = 1, 9, 12), respectively. As the hydrogen molecules are dissociatively adsorbed on Co_6 (up to a maximum of four molecules), an electronic band with hydrogen character develops in the deepest region (high binding energies) of the DOS spectrum; see the sequence from Co_6 to $2H@Co_6$ in Fig. 4, and then $(8H+nH_2)@Co_6$ with n=0,1,9 and 12 in Fig. 12. Each H atom of the dissociated molecules adds one spin up and one spin down states to this band, but contributes with one electron only. Therefore, one of those H-like states has to be filled with one electron transferred by the Co cluster. The H levels hybridize with the deepest up and down states of cobalt. Panel (a) of Fig. 13 shows the wave functions of the four deepest electronic levels with spin up character of $2H@Co_6$. The first three show H-Co hybridization, and the fourth presents pure Co character. In $nH@Co_6$ (n=2,4,6,8), the spin down states of the H band, hybridized with one level of the Co cluster, lie in the region between -7.8 eV and -3.2 eV, well separated from the pure Co band. The H-like spin up levels appear also above -7.8 eV, but are extended into a broader energy region than the spin down levels, and are intermixed with the Co levels.

Starting with $(8H+H_2)@Co_6$ a deep band with character of molecular hydrogen develops below -7.8 eV as H_2 molecules are added; this band, at the left of the thick vertical line in the panels of Fig. 12, is well separated from the other bands. The wave function of the deepest spin up state in $(8H+H_2)@Co_6$ is shown in panel (b) of Fig. 13. This wave function has H_2 character. Each added H_2 molecule contributes with one spin up and one spin down levels to the new band in the $(8H+mH_2)@Co_6$ clusters. With increasing coverage, the band of hybridized atomic H-like levels shrinks a little, and the band of molecular hydrogen levels broadens, extending between -10.5 eV and -6.8 eV. These two bands do not mix and remain well separated.

In summary, the evolution of the spin up and the spin down DOS of Co_6, as the cluster is progressively saturated with hydrogen, can be understood by the combined effects of two facts: 1) the transfer of electrons from the levels in the vicinity of the Fermi level to the spin down states introduced by atomic hydrogen, and 2) the stabilization of the states with spin down of the cobalt cluster as levels with molecular hydrogen character are introduced in the deepest part of the spectrum. Thus some spin up electrons of the Co cluster are transferred to the spin down states that cross below the Fermi energy. These two effects tend to lower the magnetic moment of the cluster with increasing hydrogen coverage and consequently the spin up and spin down DOS tends to be more symmetric. Finally the system reaches a compensated spin state, that is with equal DOS for electrons with spin up and spin down, at full hydrogen coverage, $(12H_2+8H)@Co_6$. Moreover this cluster exhibits a closed shell electronic structure, with a significant HOMO-LUMO gap of 1.03 eV, what correlates with the fact that this cluster is fully saturated with hydrogen and no more hydrogen can be adsorbed into the system.
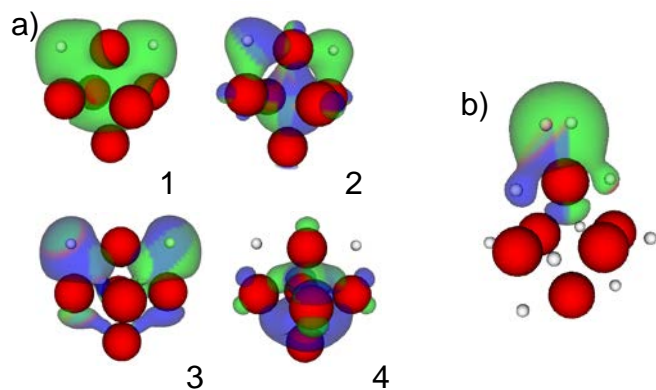
Figure 13. a) Wave functions of the four deepest electronic states with up spin of $2H@Co_6$. States 1 to 3 correspond to the two H levels introduced by the dissociated hydrogen molecule hybridized with the deepest level of Co_6. State 4 belongs clearly to the Co_6 cluster. Similar wave functions are obtained for the spin down electrons. b) Wave function of the deepest energy state of $(8H+H_2)@Co_6$; it has H_2 character. The red balls represent the Co atoms and the little grey balls the hydrogen atoms.

The dissociation of free molecular hydrogen is a highly endothermic process (dissociation energy = - 4.75 eV). However, as it has been shown in the previous sections, molecular hydrogen can dissociate on the surface of clean cobalt clusters and also on cobalt clusters preloaded with dissociated hydrogen, since the clusters act as catalysts for the dissociation process. Table 3 gives the dissociation energy of H_2 on clean Co_6 and Co_{13} and on the clusters preloaded with one dissociated H_2 molecule. The hydrogen dissociation energies are calculated as the energy difference between the energy of the cluster with H_2 adsorbed in the molecular form minus the energy of the cluster with H_2 adsorbed in the dissociated form. All the energies are positive what shows that hydrogen dissociation on cobalt clusters is an exothermic process. Small activation energies for dissociation are expected based on the experimentally determined[58] activation energy for adsorption on unsupported cobalt catalysts (58 meV).

Table3. Dissociation energy of H_2 on Co_6 and Co_{13}, clean and preloaded with one dissociated H_2 molecule. See text for details and definitions. The calculated and experimental, in parenthesis, dissociation energy of free H_2 has been included for comparison.

cluster	$E_{dissociation}$ [H_2] (eV)
Free H_2 (experimental)	-4.59 (-4.75)
Co_6	0.48
$2H@Co_6$	1.06
Co_{13}	1.02
$2H@Co_{13}$	0.91

An alternative pathway to saturate Co_6 with hydrogen consists in the sequential adsorption of hydrogen in molecular form only. It can be expected that deposition at low temperature and very low kinetic energies may allow H_2 to stay in molecular

form, because under these restrictive conditions the molecule will not be able to surpass the dissociation barrier. Thus, starting with $2H_2@Co_6$ we have explored the initial stages of the saturation process by adding up to a total of eight hydrogen molecules. The first six molecules sequentially adsorb on top of the six Co atoms of the cluster (see Fig. 14). Beginning with the seventh molecule, the Co atoms adsorb two molecules. Evidently, the configurations with all the H_2 adsorbed in the molecular form are less stable than the alternative ground state structures presented above. The adsorption energies of each new molecule added along the molecular adsorption pathway, and the average adsorption energies per molecule at each stage are given in Table 2. Also shown in the table are the magnetic moments of the complexes. Although adsorption of the first molecule preserves the magnetic moment of the cobalt cluster, adsorption of additional H_2 results in a more pronounced drop of the magnetic moment compared to the lowest energy adsorption channel
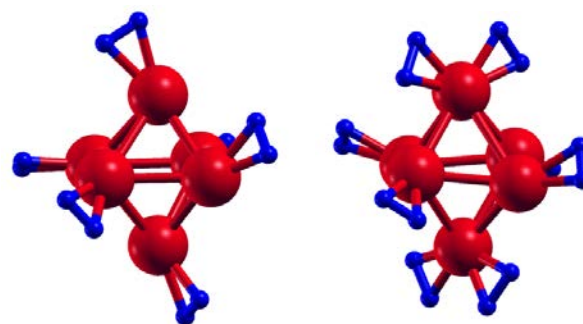

Figure 14. Molecular adsorption of six and eight H_2 molecules on Co_6.

It becomes interesting to compare the results presented above with the adsorption of hydrogen on Pd_6, which also has the octahedral structure, being Pd, on the other hand, a metal of the 4d series. Adsorption of hydrogen on Pd clusters has been studied[18-20,55,58] because experiments indicate that doping of porous carbons with Pd clusters enhances the hydrogen adsorption capacity of the material.[17] The most stable channel for the adsorption of the first H_2 molecule on free Pd_6 is also the dissociative chemisorption of the molecule.[59] At variance with the case of Co_6, the two H atoms chemisorb on the centers of two opposite triangular faces of Pd_6. Additional H_2 molecules also dissociate, up to a maximum of seven molecules. The chemisorption of hydrogen affects the structure of the host Pd_6 cluster, which changes with every new adsorbed molecule. The octahedral structure, however, is recovered when the cluster hosts six and seven dissociated molecules. When additional H_2 is deposited, molecular adsorption is the only stable channel of those molecules and the cluster adsorbs up to six more molecules. Pd_6 becomes saturated with thirteen molecules, seven dissociated and six in molecular form. In summary, Co_6 adsorbs more hydrogen, and being lighter it holds promise as a dopant of porous carbons. In

fact, with 32 adsorbed atoms (12 H_2 molecules and 8 H atoms) the ideal hydrogen storage capacity of Co_6 amounts to 8.4 % in weight.

Conclusions

The interaction of hydrogen with transition metal clusters and nanoparticles is of fundamental interest in a variety of fields and technological applications such as hydrogenation reactions, hydrogen fuel cells and hydrogen storage. With this motivation, the adsorption and dissociation of molecular hydrogen on Co_6 and Co_{13} has been investigated using the Density Functional formalism. For Co_6 we find an octahedron as the minimum energy structure in agreement with previous calculations. For Co_{13} we found that the lowest energy configuration is formed by two (1,1,1) layers of the fcc lattice with 7 and 6 atoms each, respectively. H_2 can adsorb on the cobalt clusters following two channels: molecular adsorption and dissociative chemisorption. For the two clusters investigated the dissociative chemisorption of the first H_2 molecule is the preferred channel. Each individual hydrogen atom sits above a Co-Co bond in a region of enhanced electronic density forming a kind of ionic bond with the cluster, like in metal hydrides. On the other hand, H_2 can be adsorbed also as a molecule on top of a Co atom with a relatively weak covalent type of bonding involving polarization of the electronic charge of the molecule. The molecular adsorption of one H_2 molecule does not change the magnetic moment of the cluster, whereas the dissociative chemisorption of H_2 reduces the magnetic moment of the cluster in two units.

Saturation of Co_6 with hydrogen has been studied through sequential addition of H_2. The first four hydrogen molecules dissociate, leading to $8H@Co_6$. Additional hydrogen does not dissociate and it is adsorbed in molecular form. Up to 12 additional H_2 molecules can be adsorbed on top of $8H@Co_6$ leading to the saturated structure $(8H+12H_2)@Co_6$. The magnetic moment is progressively reduced with increasing hydrogen content and is quenched down to zero in the saturated cluster, $(8H+12H_2)@Co_6$. The electronic states of the dissociated hydrogen are located in the bottom part of the spectrum of Co states and are partially hybridized with the deepest energy levels of Co. In contrast, hydrogen adsorbed in the molecular form leads to an electronic band well below the Co levels. This band has molecular hydrogen character and is not hybridized with the Co states.

In summary our calculations have clarified the mechanisms of the interaction between hydrogen and cobalt clusters, and the competition between molecular and dissociative adsorption of H_2. This study suggests the possibility of widening the applications of cobalt clusters in a variety of fields. Moreover, the adsorption of hydrogen allows controlling the magnetism of the clusters. Saturation of Co clusters with hydrogen leads to 8.4% content of hydrogen in weight, what is promising for hydrogen storage.

Conflicts of interest

There are no conflicts to declare.

Acknowledgements

References

1   W. D. Knight, K. Clemenger, W. A. de Heer, W. A. Saunders, M. Y. Chou and M. L. Cohen, Electronic shell structure and abundances of sodium clusters. *Phys. Rev. Lett.*, 1984, **52**, 2141-2143.
2   C. Baladrón and J. A. Alonso, Stability and magic numbers of hetero-atomic clusters of simple metals. *Physica B*, 1988, **154**, 73-81.
3   J. A. Alonso, Electronic and atomic structure, and magnetism of transition metal clusters. *Chem. Rev.*, 2000, **100**, 637-677.
4   J. M. Montejano-Carrizales, M. P. Iñiguez, J. A. Alonso and M. J. López, Theoretical study of icosahedral Ni clusters within the embedded atom method. *Phys. Rev. B*, 1996, **54**, 5961-5969.
5   W. Zhang, W-C. Lu, Q-J. Zang, C. Z. Wang and K. M. Ho, Bulklike structures for medium-sized Al_n (n=31–40) clusters. *J. Chem. Phys.*, 2009, **130**, 144701.
6   A. Lechtken, Ch. Neiss, M. M. Kappes and D. Schooss, Structure determination of gold clusters by trapped ion electron diffraction: Au_{14}^- - Au_{19}^-. *Phys. Chem. Chem. Phys.*, 2009, **11**, 4344–4350.
7   G. L. Gutsev, C. W. Weatherford, K. G. Belay, B. R. Ramachandran and P. Jena, An all-electron density functional theory study of the structure and properties of the neutral and singly charged M12 and M13 clusters: M = Sc-Zn. *J. Chem. Phys.*, 2013, **138**, 164303.
8   E. Kim, A. Mohrland, P. F. Weck, T Pang, K. R. Czerwinski and D. Tománek, Magic numbers in small iron clusters: A first-principles study. *Chem. Phys. Lett.*, 2014, **613**, 59-63.
9   J. Souto-Casares, M. Sakurai and J. R. Chelikowsky, Structural and magnetic properties of large cobalt clusters. *Phys. Rev. B*, 2016, **93**, 174418.
10 M. J. Piotrowski, C. G. Ungureanu, P. Tereshchuk, K. E. A. Batista, A. S. Chaves, D. Guedes-Sobrinho and J. L. F. Da Silva, Theoretical study of the structural, energetic, and electronic properties of 55-atom metal nanoclusters: A DFT investigation within van der Waals corrections, spin−orbit coupling, and PBE+U of 42 metal systems. *J. Phys. Chem. C*, 2016, **120**, 28844-28856.
11 C. Di Paola, R. D'Agosta and F. Baletto, Geometrical effects on the magnetic properties of nanoparticles. *NanoLetters*, 2016, **16**, 2885-2889.
12 E. K. Parks and S. J. Riley, Nickel cluster structure determined from the adsorption of molecular nitrogen: Ni_{49}-Ni_{71}. *Z. Phys. D*, 1995, **33**, 59-76.
13 F. Calle-Vallejo, J. I. Martínez, J. M. García-Lastra, Ph. Sautet and D. Loffreda, Fast prediction of adsorption properties for platinum nanocatalysts with generalized coordination numbers. *Angew. Chem. Int. Ed.*, 2014, **563**, 1-5.
14 G. Yushin, R. Dash, J. Jagiello, J. E. Fischer and Y. Gogotsi, Carbide-derived carbons: Effect of pore size on hydrogen

uptake and heat of adsorption. *Adv. Funct. Mater.*, 2006, **16**, 2288-2293.

15 R. T. Yang, Hydrogen storage by alkali-doped carbon nanotubes–revisited. *Carbon*, 2000, **38**, 623-641.

16 A. D. Lueking and R. T. Yang, Hydrogen spillover to enhance hydrogen storage-Study of the effect of carbon physicochemical properties. *Appl. Catal. A*, 2004, **265**, 259–268.

17 C. I. Contescu, C. M. Brown, Y. Liu and V. V. Bhat, Detection of hydrogen spillover in palladium modified activated carbon fibers during hydrogen adsorption. *J. Phys. Chem. C*, 2009, **113**, 5886-5890.

18 A. W. Pelzer, J. Jellinek and K. Jackson, H_2 saturation on palladium clusters, *J. Phys. Chem. A*, 2015, **119**, 3594–3603.

19 M. J. López, I. Cabria and J. A. Alonso, Palladium clusters anchored on graphene vacancies and their effect on the reversible adsorption of hydrogen. *J. Phys. Chem C*, 2014, **118**, 5081-5090.

20 M. Blanco-Rey, J. I. Juaristi, M. Alducin, M. J. López and J. A. Alonso, Is spillover relevant for hydrogen adsorption and storage in porous carbons doped with palladium nanoparticles? *J. Phys. Chem. C*, 2016, **120**, 17357–17364.

21 S. R. Liu, H. K. Zhai and L. S. Wang, Electronic and structural evolution of Co_n clusters (n=1 – 108) by photoelectron spectroscopy. *Phys. Rev. B*, 2001, **64**, 153402.

22 I. M. L. Billas, A. Chatelain and W. D. De Heer, Magnetism of Fe, Co and Ni clusters in molecular beams. *J. Mag. Mag. Mater.*, 1997, **168**, 64-84.

23 Q-M. Ma, Z. Xie, J. Wang, Y. Liu and Y-C. Li, Structures, stabilities and magnetic properties of small Co clusters, *Phys. Lett. A*, 2006, **358**, 289–296.

24 S. Datta, M. Kabir, S. Ganguly, B. Sanyal, T. Saha-Dasgupta, and A. Mookerjee, Structure, bonding, and magnetism of cobalt clusters from first-principles calculations. *Phys. Rev. B*, 2007, **76**, 014429.

25 A. Sebetci, Cobalt clusters (Co_n, n ≤ 6) and their anions. *Chem. Phys.*, 2008, **354**, 196–201.

26 F. Aguilera-Granja, A. Vega and L. C. Balbás, A new family of star-like icosahedral structures for small cobalt clusters. *Chem. Phys.*, 2013, **415**, 106–111.

27 A. K. Kandalam, B. Kiran, P. Jena, X. Li, A. Grubisic and K. H. Bowen, Ground state structures and photoelectron spectroscopy of [Co_m(coronene)]⁻ complexes. *J. Chem. Phys.*, 2007, **126**, 084306.

28 T. Alonso-Lanza, A. Ayuela and F. Aguilera-Granja, Chemical bonding of transition-metal Co_{13} clusters with graphene. *Chem. Phys. Chem.*, 2015, **16**, 3700 – 3710.

29 T. Alonso-Lanza, A. Mañanes and A. Ayuela, Interaction of cobalt atoms, dimers, and Co_4 clusters with circumcoronene: A theoretical study. *J. Phys. Chem. C*, 2017, **121**, 18900–18908.

30 A. M. Saib, M. Claeys and E. van Steen, Silica supported cobalt Fischer–Tropsch catalysts: effect of pore diameter of support. *Catal. Today*, 2002, **71**, 395-402.

31 H. Schulz, Z. Nie and F. Ousmanov, Construction of the Fischer–Tropsch regime with cobalt catalysts. *Catal. Today*, 2002, **71**, 351-360.

32 J. M. Zowtiak, D. Gordon, G. D. Weatherbee and C. H. Bartholomew, Activated adsorption of H_2 on cobalt and effects of support thereon. *J. Catal.*, 1983, **82**, 230-235.

33 K. M. E. Habermehl-Cwirzen, K. Kauraala and J. Lahtinen, Hydrogen on cobalt: The effects of carbon monoxide and sulphur additives on the D_2/Co(0001) system. Phys. Scripta T, 2004, **108**, 28–32.

34 W. Lisowski, Kinetics and thermodynamics of hydrogen interaction with thin cobalt films. *App. Surf. Sci.*, 1989, **35**, 399-408.

35 K. H. Ernst, E. Schwarz and K. Christmann. The interaction of hydrogen with a cobalt (1010) surface. *J. Chem. Phys.*, 1994, **101**, 5388-5401.

36 D. J. Klinke and L. J. Broadbelt. A theoretical study of hydrogen chemisorption on Ni(111) and Co(0001) surfaces. *Surf. Sci.*, 1999, **429**, 169-177.

37 P. van Helden, J. A. van den Berg and C. J. Weststrate, Hydrogen adsorption on Co surfaces: A density functional theory and temperature programmed desorption study. *ACS Catal.*, 2012, **2**, 1097-1107.

38 I. Swart, F. M. F. de Groot, B. M. Weckhuysen, P. Gruene, G. Meijer, and A. Fielicke, H_2 adsorption on 3d transition metal clusters: A combined infrared spectroscopy and density functional study. *J. Phys. Chem. A*, 2008, **112**, 1139-1149.

39 M. D. Morse, M. E. Geusic, J. R. Heath, and R. E. Smalley, Surface reactions of metal clusters. II. Reactivity surveys with D_2, N_2, and CO. *J. Chem. Phys.*, 1985, **83**, 2293-2304.

40 J. Ho, L. Zhu, E. K. Parks, and S. J. Riley, Temperature dependence of the reactions of small cobalt clusters with deuterium. *J. Chem. Phys.*, 1993, **99**, 140-147.

41 F. Liu and P. B. Armentrout, Guided ion-beam studies of the kinetic-energy-dependent reactions of Co^+_n (n=2-16) with D_2: Cobalt cluster-deuteride bond energies. *J. Chem. Phys.*, 2005, **122**, 194320.

42 A. Nakhaei Pour, J. Karimi, Z. Keyvanloo and M. Hashemian, Size dependence adsorption of hydrogen on cobalt clusters: A DFT study. *J. Nano Research*, 2016, **42**, 100-111.

43 N. O. Jones, M. R. Beltran, S. N. Khanna, T. Baruah and M. R. Pederson, Hydrogen adsorption and magnetic behavior of Fe_n and Co_n clusters: Controlling the magnetic moment and anisotropy one atom at a time. *Phys. Rev. B*, 2004, **70**, 165406.

44 A. Franczak, F. Bohr, A. Levesque and J. P. Chopart, Quantum chemical study of hydrogen evolution during cobalt electrodeposition. *Res. Rev. J. Chem.*, 2015, **4 (4)**, 75-86.

45 F. Buendía and M. R. Beltran, Theoretical study of hydrogen adsorption on Co clusters. *Comput. Theoret. Chem.*, 2013, **1021**, 183–190.

46 See <https://wiki.fysik.dtu.dk/dacapo> for a description of the total energy DACAPO code, based on the Density Functional Theory, 2009.

47 D. Vanderbilt, Soft self-consistent pseudopotentials in a generalized eigenvalue formalism. *Phys. Rev. B*, 1990, **41**, R7892-7895.

48 J. P. Perdew and Y. Wang, Accurate and simple analytic representation of the electron-gas correlation energy. *Phys. Rev. B*, 1992, **45**, 13244-13249.

49 H. Monkhorst and J. Pack, Special points for Brillouin-zone integration. *Phys. Rev. B*, 1976, **13**, 5188–5192.

50 A.D. Becke, Density-functional exchange-energy approximation with correct asymptotic behavior, *Phys. Rev. A*, 1988, **38**, 3098-3100.

51 C. Lee, W. Yang and R.G. Parr, Development of the Colie-Salvetti correlation-energy formula into a functional of the electron density, *Phys. Rev. B*, 1988, **37**, 785-789.

52 J. P. Perdew, K. Burke and M. Ernzerhof, Generalized gradient approximation made simple, *Phys. Rev. Lett.*, 1996, **77**, 3865-3868.

53 M. B. Knickelbein, Magnetic moments of bare and benzene-capped cobalt clusters. *J. Chem. Phys.*, 2006, **125**, 044308.

54 X. Xu, S. Yin, R. Moro and W. de Heer, Magnetic moments and adiabatic magnetization of free cobalt clusters, *Phys. Rev. Lett.*, 2005, **95**, 237209.

55 I. Cabria, M. J. López, S. Fraile and J. A. Alonso, Adsorption and dissociation of molecular hydrogen on palladium clusters supported on graphene, *J. Phys. Chem. C*, 2012, **116**, 21179–21189.

56 J. A. Alonso, Structure and properties of atomic nanoclusters. 2nd edition. Imperial College Press, London, 2012.

57 I. V. Yudanov, A. Genest, S. Schauermann, H.-J. Freund and N. Rösch, Size dependence of the adsorption energy of CO on metal nanoparticles: A DFT search for the minimum value. *Nanoletters*, 2012, **12**, 2134-2139.

58 J. M. Zowtiak and C. H. Bartholomew, The kinetics of H2 adsorption and desorption from cobalt and the effects of support thereon. Journal of Catalysis, 1983, **83**, 107-120.

59 A. Granja-DelRío, J. A. Alonso and M. J. López, Steric and chemical effects on the hydrogen adsorption and dissociation on free and graphene-supported palladium clusters. *Comput. Theoret. Chem.*, 2017, **1107**, 23-29.